



Queensland University of Technology
Brisbane Australia

This may be the author's version of a work that was submitted/accepted for publication in the following source:

[Krishnakanth, Pushpanjali, Schmutz, Beat, Steck, Roland, Mishra, Sanjay, Schuetz, Michael, & Epari, Devakar](#)

(2011)

Can the contra-lateral limb be used as a control with respect to analyses of bone remodelling?

Medical Engineering and Physics, 33(8), pp. 987-992.

This file was downloaded from: <https://eprints.qut.edu.au/41410/>

© Consult author(s) regarding copyright matters

This work is covered by copyright. Unless the document is being made available under a Creative Commons Licence, you must assume that re-use is limited to personal use and that permission from the copyright owner must be obtained for all other uses. If the document is available under a Creative Commons License (or other specified license) then refer to the Licence for details of permitted re-use. It is a condition of access that users recognise and abide by the legal requirements associated with these rights. If you believe that this work infringes copyright please provide details by email to qut.copyright@qut.edu.au

License: Creative Commons: Attribution-Noncommercial-No Derivative Works 2.5

Notice: *Please note that this document may not be the Version of Record (i.e. published version) of the work. Author manuscript versions (as Submitted for peer review or as Accepted for publication after peer review) can be identified by an absence of publisher branding and/or typeset appearance. If there is any doubt, please refer to the published source.*

<https://doi.org/10.1016/j.medengphy.2011.03.011>

**Can the contra-lateral limb be used as a preoperative control with
respect to analyses of bone remodelling?**

P. Krishnakanth, B. Schmutz, R. Steck, S. Mishra, M.A. Schütz, D.R. Epari

Institute of Health and Biomedical Innovation, Queensland University of Technology,
Brisbane, Australia

Corresponding Author

Dr. Devakar Epari
Institute of Health and Biomedical Innovation
Queensland University of Technology
60 Musk Ave
Kelvin Grove, 4059
Australia
+61 7 3138 0167
d.epari@qut.edu.au

Introduction

Bone has the capability to adapt to changes in its mechanical loading through a process of remodelling [1]. Bone remodelling is a lifelong process whereby old bone is replaced by new bone [2]. In adults, approximately 18% of the bony skeleton is replaced annually [3]. Remodelling leads to both changes in the density and structure of bone [4].

Physical exercise is known to cause changes in the structure of bone [5]. For example, increased bone mass may be seen in the dominant arm of a tennis player [6]. In this case, the remodelling may be considered positive as it enables the individual to withstand greater limb loading. However, in instances such as fracture fixation, load-sharing with an implant may lead to unloading of the bone, a phenomenon known as stress protection, and result in undesirable bone loss [7]. This bone loss may lead to complications such as screw loosening leading to implant failure or even re-fracture [8]. In order to predict bone remodelling related to a particular treatment or implant, it is necessary to understand the mechanism of remodelling. To do this, changes in the loading conditions of the bone must be related to remodelling changes and relationships formulated. Thus, the first step in this approach is to quantify the remodelling changes.

Calculating the changes due to remodelling requires bone density distributions to be quantified prior to intervention and at a subsequent time-point providing sufficient time for remodelling changes to occur. Quantitative bone density distributions can be determined from computed tomography (CT) scans calibrated with a bone phantom [9]. Since a CT scan exposes the subject to ionising radiation, performing a CT scan on humans is considered only when it is deemed essential to form a diagnosis. Additionally, metal implants can cause artefacts rendering CT data unusable for quantitative analysis. Therefore obtaining data from human volunteers for the purpose of quantifying bone

remodelling is excluded. Alternatively, large animals (such as sheep) are commonly used in orthopaedic research [10-12] and obtaining post-mortem CT scans of bones with implants removed is commonplace. Therefore, large animals may be considered a suitable model to study implant related changes due to bone remodelling. However, obtaining pre-operative CT scans of live animals is often not possible due to the limited availability of CT scanners outside the clinical environment. An alternative approach to using a pre-operative scan of the same limb may be to use the contra-lateral limb.

Although the contra-lateral limb has been used previously as a pre-operative control for quantifying bone density changes [13-17], it may not be automatically assumed that the contra-lateral bone represents the pre-operative condition of the operated bone as this approach has not yet been validated. There may be differences in geometry and density between left and right which would make such an assumption invalid, particularly as density changes are quantified on a smaller scale. The use of the contra-lateral bone as a pre-operative control has therefore to be validated.

The goal of this study was to determine whether the contra-lateral bone may be used as a pre-operative control with respect to analyses of implant induced bone remodelling in sheep. To address this question, firstly the extent of anatomical similarity between left and right ovine tibias was investigated. In the second part of this study, the magnitude of implant related bone-remodelling is quantified to demonstrate that it is an order of magnitude greater than the inherent contra-lateral differences and thus demonstrate the capability to use the contra-lateral limb to determine patterns of bone remodelling.

Materials and Methods

Comparison of left and right tibia

Eight pairs of ovine tibia were used to determine the inherent geometric and density differences between left and right bones. The mean age of the sheep was 5.7 years (ranging from 4 years to 7 years) while the mean weight was 39.6 kg. Specimens were obtained from animals that had previously undergone a procedure on their right femur (multi-fragmentary fracture and soft-tissue injury in the distal third of the femoral diaphysis stabilized with an internal plate fixation device). Four weeks after the procedure, animals were sacrificed and the left and right tibiae were harvested.

The tibiae (both left and right placed end-to-end) were scanned using a Philips Brilliance 64 CT scanner with 120 kVp and a slice spacing of 0.67 mm resulting in a voxel size of 0.41×0.41×0.67 mm. The long axis of the tibiae was visually aligned with the long axis of the CT scanner. The bones were scanned together with a bone phantom (European Forearm Phantom (EFP), QRM GmbH, Moehrendorf, Germany) to enable conversion of Hounsfield Units (HU) to Bone Mineral Density (BMD). The images were reconstructed using a sharp convolution kernel and saved in the DICOM format.

The DICOM files of each bone pair were read into AMIRA software environment (Visage Imaging GmbH, Berlin, Germany) where the left and right bones were cropped and saved separately. In order to determine the geometric and density differences between the left and the corresponding right tibia, the right tibia was mirrored. Surface (polygon) models of the outer contour of the tibia pairs were created first using a single intensity threshold (200 HU) followed by manual segmentation in order to smooth the edges of the outer contour. The surfaces of the paired tibiae were then positioned in the same orientation by registering the surfaces of both bones with a reference bone in the

desired orientation using RAPIDFORM (INUS Technology, Seoul, Korea). (N.B. It is necessary to have all bones in the same orientation for the division into anatomical quarters required for the density comparison.) The re-alignment was performed in two steps. Firstly, a gross alignment was performed by manually selecting five corresponding points on distinct anatomical features. This was followed by a fine alignment using the Iterative Closest Point (ICP) algorithm which uses an automatic selection of points during the registration process [18].

Geometric comparison

Following alignment, the distance from the outer surface of one tibia to the other (shell-to-shell deviation) was measured in RAPIDFORM. In this procedure, the difference between the two surfaces is quantified on a point-to-point basis. The average shell-to-shell deviation was determined for the three anatomical regions; the diaphysis and proximal and distal regions (Figure 1). The diaphyseal region is determined according to the AO Principles of Fracture Management [19] that defines the proximal and distal end segments as a square whose sides are the same length as the widest part of the epiphysis and the diaphysis forms the remainder.

Bone density comparison

The transformation matrix calculated to align the two tibial surfaces previously was then applied to align the original DICOM data for the left and right tibia pairs. This transformation reorients the bones in the desired orientation. As a result of the transformation, the orientation of the CT slices is not perpendicular to the long axis of the bone. Therefore, re-slicing of the DICOM data is necessary before comparison. The density comparison was then performed using a MATLAB program developed in-house (The Mathworks, Inc, USA). The DICOM data in the diaphyseal region of each bone was

first divided into discrete volumes, defined by a quarter (i.e. medial, lateral, anterior, and posterior) of a transverse slice (Figure 2). Conversion of HU values to bone mineral density (BMD) was performed using a relationship between the HU values and apparent density of hydroxyapatite determined from the bone phantom. The average BMD in each volume was then calculated and the percentage difference between corresponding volumes of the left and right tibia pairs were computed. Only BMD values corresponding to cortical bone, with an intensity value greater than 600 HU [20] were considered in the analysis.

Comparison of operated and intact contra-lateral tibia

Specimens were obtained from a parallel study which is only briefly described here. Eight sheep underwent a mid-diaphyseal osteotomy of the right tibia to create a segmental defect (3 cm). The defect was stabilised with a compression plate (7-hole DCP, Synthes AG, Switzerland). Animals were sacrificed 3 months after surgery and the fractured and intact contra-lateral tibia were CT scanned together with a bone phantom. A density comparison between the fractured and intact pairs (n=8) was performed using the procedures described above. Newly formed bone as part of the healing process (i.e. callus) was not considered in the analysis. In order to quantify localised bone density changes the peak (maximum) percentage density difference in regions in close proximity to screw holes and the segmental defect was calculated.

Results

Comparison of left and right tibia

Geometry comparison

The differences from the outer surface one tibia to the other, for the whole tibia and the different regions separately, are listed in Table 1 for all tibia pairs. Seven out of eight pairs had a difference of less than 1 mm for over 90% of the measured points and in the diaphyseal region six out of eight pairs had a difference of less than 1 mm for all of the measured points.

The average geometric difference [mean (min - max)] between the entire outer surfaces of the tibiae was determined to be 0.37 (0.29 - 0.48) mm. The average deviation for the diaphyseal regions was 0.27 (0.16 - 0.37) mm. In the distal and proximal segments the average geometric differences were 0.57 (0.32 - 1.11) mm and 0.36 (0.29 - 0.46) mm respectively. Figure 1 shows the deviation between the outer surfaces of left and right tibiae for one of the pairs.

Density comparison

The left and right density differences [mean (max)] in the diaphyseal region of the tibiae were 2.26% (8.21) medially, 3.71% (8.25) posteriorly, 2.67% (10.77) anteriorly and 2.75% (7.57) laterally for all eight pairs. Whilst the maximum density difference between a left and corresponding right quarter was 10.77%, the majority (over 90% of investigated quarters) had density differences of less than 5% (Figure 3).

Comparison of operated and intact contra-lateral tibia

The percentage density difference between an operated and intact pair for each of the four quarters along the length of the diaphysis is shown in Figure 4. The density differences were not uniform distributed but rather in close proximity to the segmental defect and the location of screw holes from the implant. The maximum density differences (up to 50%) occurred in close proximity to the segmental defect and in regions in close proximity to the screw holes (up to 30%). The peak density differences adjacent to the segmental defect and the screw holes are shown in Figure 5.

Discussion

The goal of this study was to determine whether the contra-lateral bone may be used as a pre-operative control with respect to analyses of implant induced bone remodelling in sheep. To address this question, firstly the extent of anatomical similarity between left and right ovine tibias was investigated. In the second part of this study, the magnitude of implant related bone-remodelling is quantified to demonstrate that it is an order of magnitude greater than the inherent contra-lateral differences and thus demonstrate the capability to the use the contra-lateral limb to determine patterns of bone remodelling.

The investigation of anatomical similarity began with an examination of the geometric similarity. The extent of geometric similarity between left and right bones was not consistent across the three regions examined. While the diaphyseal and proximal regions showed good similarity with average differences less than 0.5 mm, the distal regions of the bone showed average differences of up to 1 mm. The similarity for each of

the different regions is partly explained by the alignment procedure used. Because of the larger surface area of the proximal region, this results in a larger number of points from this region that are used in the ICP algorithm for alignment. Therefore, there is an alignment bias towards the proximal end. Much of the disparity between the surfaces at the distal end can be attributed to length differences between left and right tibia. Since the focus in this study, was on the diaphyseal region of the tibia, in which 99% (92 – 100) of the measured points had a surface deviation of less than 1 mm, the left and right tibia can be considered to have a high degree of geometric similarity in the diaphysis.

A density comparison of the left and right tibiae was then conducted by dividing the diaphyseal region of the bone into quarters (medial, lateral, anterior and posterior). The majority of quarters (over 90%) yielded density differences of less than 5%. The maximum difference determined between corresponding left and right quarters from all pairs investigated was 10.7%; however the total percentage of quarters with a density difference of greater than 10% was less than 1%. The occurrence of larger density differences did not show any recurring pattern for the bone pairs compared.

Interestingly, the density analysis of the left and right bones found that, the right tibiae in all cases tended to have lower ($1.78\% \pm 0.371$) density values than the left. It is possible that the lower bone density in the right tibia could be the result of a surgical procedure (multi-fragmentary fracture and soft-tissue injury) that had been performed on the right femur four weeks prior sacrifice. Though loading was not monitored in these animals, it is plausible that the operated limbs were subjected to reduced weight bearing. Thus, the density comparison of left and right tibia pairs incorporates potential density changes due to reduced weight bearing and subsequent remodelling as well as the inherent bone differences. It is however unlikely that the reduced weight bearing

resulted in significant bone loss in the affected limb for two reasons. Firstly, due to the relatively short time period of four weeks and secondly, while the animals may have reduced weight bearing during normal gait through limping, the bones were not completely unloaded as the animals continued normal activities such as running, jumping, standing up and lying down, all activities that can produce high loads on the tibia. Therefore, in a worst-case where there may be some short-term effects of remodelling; the left and right density differences are of the order of 5%.

The methods applied in this study are subject to limitations. The comparison of bone density in corresponding quarters is subject to the accuracy of alignment of left and right bones. Despite the very good alignment, evident in the low geometric differences as described above, alignment between the two tibiae is not perfect primarily due to differences in tibial length. Because the height of the quarters compared (1 slice thickness = 0.67 mm) is less than the length differences (2-3 mm), the possibility exists that the compared quarters were slightly offset from one another. Analysis of the variation in bone density between neighbouring slices revealed average differences of $0.30\% \pm 0.03$ with a maximum difference from all eight pairs of 1.9%. As the difference between adjacent quarters (approx 0.5%) is an order of magnitude lower than the left and right differences (approx 5%), an axial misalignment of one or two slices is unlikely to yield observable differences. Figure 6 shows the percentage difference in density between adjacent slices of a tibia for the length of the diaphysis.

The method to align the tibia in the same orientation requires a transformation followed by re-slicing. The re-slicing requires an interpolation of the DICOM data to determine values for voxels in the re-sliced data that are located between the original

voxel positions. Since there is a high degree of similarity in density between adjacent slices, the effects of this interpolation are expected to be minimal.

Segmentation of the CT data to define the outer and inner surfaces of the cortex of the tibia is subject to selection of an appropriate threshold value. Due to partial volume effects (PVE) in CT datasets, which occur predominantly in border regions where bone and soft tissue interface, a voxel spanning this region contains a mixture of tissue types [21] and the Hounsfield Unit stored in that voxel is an average of the included tissues. This makes a clear determination of the bone boundary difficult. While this artefact cannot be eliminated, by scanning both paired tibiae in a single CT scan and then creating models from these scans with the same intensity threshold, the two bones are treated equally and the effects of over or under-estimating the cortical boundary cancel out in both the geometric and density comparison.

Thus far this study has demonstrated that left and right tibial pairs have a high degree of geometric similarity and comparable density distributions. For the contra-lateral bone to be considered an appropriate control to quantify bone remodelling, it must second be demonstrated that the density changes as a result of remodelling are substantially greater than any left-right differences. A comparison of operated (3 months post-surgery) and intact contra-lateral tibia showed substantially larger density differences compared to those determined in the left-right comparison.

The greatest density changes (bone loss) as a result of the osteotomy and plate fixation were seen in close proximity to the segmental defect (10-50 %) and the screw holes (10-30%). The magnitude of the differences observed were substantially larger than the differences between the left and right matched pairs (5%). The location of the observed density differences between the operated and the intact contralateral tibia

where in regions influenced by the defect and plate fixation. As the plate was affixed to the medial aspect of the tibia the orientation of the screws was mostly in the medial-lateral plane. Accordingly, the bone loss adjacent to the screw holes occurred predominantly in the medial and lateral quarters.

The finding of bone loss around the screw holes is in agreement with qualitative studies [22-25] examining changes around fracture fixation implants, in which histological and radiographic techniques were used to assess bone density changes due to remodelling. Although CT data has been previously used to quantify changes due to remodelling [13], the comparison was performed using significantly larger regions (i.e. Gruen zones; divided medially and laterally and each region many slices thick) as compared to those in the present study (medial, lateral, anterior, posterior, 1 slice thick). The techniques applied in this study have further refined CT based evaluation methods by increasing their resolution which will be useful in quantifying highly localized remodelling changes such as those occurring as a result of fracture fixation.

In summary, left and right ovine tibiae were found to have a high degree of geometric similarity with differences of less than 1.0 mm in surface deviation and density difference of less than 5% in the diaphyseal region. The density differences occurring as a result of implant related bone remodelling (10-40%) were well above the observed contra-lateral differences. Although recent studies in small animal models have produced conflicting results as to whether remodelling effects are confined to the bone subjected to external loading or whether the contra-lateral is affected through systemic neuronal pathways [26, 27], in this study localized implant related remodelling produced substantial differences with respect to the contra-lateral bone.

Hence, it can be concluded that for the purposes of implant related bone remodelling investigations in sheep, the intact contra-lateral tibia may be considered an alternative to a pre-operative control, provided that the changes in density due to remodelling yield differences greater than 5% and including a margin of safety, only changes greater than 10% should be considered as a result of remodelling. Although limited to the diaphyseal region and only to the cortical bone, this method may be used to quantify the pattern of bone remodelling in experimental situations. The quantified patterns of bone remodelling may then serve to validate the predictions of numerical algorithms simulating bone remodelling.

Acknowledgements

This study was partially funded by a grant from the Australian Research Council (LP0776309).

References

- [1]. Wolff J, Maquet P, Furlong R; 'The law of bone remodelling' Springer, 1986 126.
- [2]. Hadjidakis DJ, Androulakis II. Bone remodelling. *Annals of the New York Academy of Sciences* 2006;1092(Women's Health and Disease: Gynecologic, Endocrine, and Reproductive Issues):385-396.
- [3]. Ortner DJ; 'Identification of pathological conditions in human skeletal remains' Academic Press, 2003 645.
- [4]. Jang IG, Kim IY, Kwak BB. Analogy of strain energy density based bone-remodeling algorithm and structural topology optimization. *Journal of Biomechanical Engineering* 2009;131(1):1135-1150.
- [5]. Woitge HW, Friedmann B, Suttner S, Farahmand I, Muller M, Schmidt-Gayk H, Baertsch P, Ziegler R, Seibel MJ. Changes in bone turnover induced by aerobic and anaerobic exercise in young males. *Journal of Bone and Mineral Research* 1998;13(12):1797-1804.
- [6]. Kannus P, Haapasalo H, Sankelo M, Sievanen H, Pasanen M, Heinonen A, Oja P, Vuori I. Effect of starting age of physical activity on bone mass in the dominant arm of tennis and squash players. *Annals of Internal Medicine* 1995;123(1):27-31.
- [7]. Hernandez C], Keaveny TM. A biomechanical perspective on bone quality. *Bone* 2006;39(6):1173-1181.
- [8]. Augat P, Claes L. Increased cortical remodeling after osteotomy causes posttraumatic osteopenia. *Bone* 2008;43(3):539-543.
- [9]. Langton CM, Njeh CF; 'The physical measurement of bone' Institute of Physics London; 2004.
- [10]. Hallfeldt KK, Stutzle H, Puhlmann M, Kessler S, Schweiberer L. Sterilization of partially demineralized bone matrix: the effects of different sterilization techniques on osteogenetic properties. *Journal of Surgical Research* 1995;59(5):614-620.
- [11]. Viljanen VV, Gao TJ, Lindholm TC, Lindholm TS, Kommonen B. Xenogeneic moose (*Alces alces*) bone morphogenetic protein (mBMP)-induced repair of critical-size skull defects in sheep. *International Journal of Oral and Maxillofacial Surgery* 1996;25(3):217-222.
- [12]. Yuehuei HA, Friedman RJ; 'Animal models in orthopaedic research' CRC Press, 1998 604.
- [13]. Engh CA, McGovern TF, Bobyn JD, Harris WH. A quantitative evaluation of periprosthetic bone-remodeling after cementless total hip arthroplasty. *J Bone Joint Surg Am* 1992;74-A(7):1009-1020.
- [14]. Kerner J, Huiskes R, van Lenthe GH, Weinans H, van Rietbergen B, Engh CA, Amis AA. Correlation between pre-operative periprosthetic bone density and post-operative bone loss in THA can be explained by strain-adaptive remodelling. *Journal of Biomechanics* 1999;32(7):695-703.
- [15]. Lengsfeld M, Gunther D, Pressel T, Leppek R, Schmitt J, Griss P. Validation data for periprosthetic bone remodelling theories. *Journal of Biomechanics* 2002;35(12):1553-1564.
- [16]. Van Rietbergen B, Huiskes R, Weinans H, Sumner DR, Turner TM, Galante JO. ESB Research Award 1992. The mechanism of bone remodeling and resorption around press-fitted THA stems. *Journal of Biomechanics* 1993;26(4-5):369-382.
- [17]. Weinans H, Huiskes R, van Rietbergen B, Sumner DR, Turner TM, Galante JO. Adaptive bone remodeling around bonded noncemented total hip arthroplasty: a comparison between animal experiments and computer simulation. *Journal of Orthopaedic Research* 1993;11(4):500-513.

- [18]. Lee YS, Seon JK, Shin VI, Kim GH, Jeon M. Anatomical evaluation of CT-MRI combined femoral model. *Biomedical Engineering Online* 2008;7:12.
- [19]. Ruedi TP, Murphy WM; 'AO Principles of fracture management' Vol 2; AO Publishing, Davos Platz; 2001.
- [20]. Rathnayaka K, Sahama T, Schuetz MA, Schmutz B. Effects of CT image segmentation methods on the accuracy of long bone 3D reconstructions. *Medical Engineering and Physics* 2011;33(2):226-33.
- [21]. Jiri J; 'Medical Image processing, reconstruction and restoration: concepts and methods' Taylor & Francis Group, 2006.
- [22]. Claes L. The mechanical and morphological properties of bone beneath internal fixation plates of differing rigidity. *Journal of Orthopaedic Research* 1989;7(2):170-177.
- [23]. Sumitomo N, Noritake K, Hattori T, Morikawa K, Niwa S, Sato K, Niinomi M. Experiment study on fracture fixation with low rigidity titanium alloy: plate fixation of tibia fracture model in rabbit. *Journal of Materials Science: Materials in Medicine* 2008;19(4):1581-1586.
- [24]. Uthoff HK, Dubuc FL. Bone structure changes in the dog under rigid internal fixation. *Clinical Orthopaedics and Related Research* 1971;81:165-170.
- [25]. Uthoff HK, Foux A, Yeadon A, McAuley J, Black RC. Two processes of bone remodeling in plated intact femora: an experimental study in dogs. *Journal of Orthopaedic Research* 1993;11(1):78-91.
- [26]. Sample SJ, Behan M, Smith L, Oldenhoff WE, Markel MD, Kalscheur VL, Hao Z, Miletic V, Muir P. Functional adaptation to loading of a single bone is neuronally regulated and involves multiple bones. *Journal of Bone and Mineral Research* 2008;23(9):1372-1381.
- [27]. Sugiyama T, Price JS, Lanyon LE. Functional adaptation to mechanical loading in both cortical and cancellous bone is controlled locally and is confined to the loaded bones. *Bone* 2010;46(2):314-321.

Figure 1: The surface deviation for a left and right tibia pair shown for each region (proximal, distal and diaphyseal). The average shell-to-shell deviation is 0.29 mm for the proximal, 0.41 mm for the distal and 0.19 mm for the diaphyseal region. Grey regions indicate a deviation of less than 1 mm.

Figure 2: The CT data is divided into four quarters (medial, lateral, anterior and posterior) for determination of density differences. Shown here are transverse cross-sections of a) intact and b) operated tibia. A compression plate was affixed medially with bicortical screws.

Figure 3: This histogram shows the distribution of analysed volumes in each of density difference ranges from the left and right (dark grey) and operated and intact comparison (light grey) for all bone pairs (n = 8).

Figure 4: Shows the percentage density difference 3 months after surgery in all four quarters (medial, lateral, anterior and posterior) along the diaphysis for a sheep tibia with segmental defect (SD) treated with a compression plate.

Figure 5: Shows the peak density difference (%) in all quarters around the screw holes and the segmental defect (SD) between the operated and intact contra-lateral tibia at 3 months.

Figure 6: Shows the percentage density difference between adjacent CT slices of a tibia in the medial quarter for one tibia pair. The lateral, anterior and posterior quarters also showed density differences of < 2% between adjacent transverse slices along the diaphyseal region of the tibia.

Table 1: Contains the average distance between the outer surfaces (shell/shell deviation) for each tibia pair for the whole tibia and for the proximal, distal and diaphyseal regions separately. Additionally, the percentage of measured points within a 1 mm tolerance is given in brackets.

Sheep	Whole tibia (mm)	Proximal (mm)	Distal (mm)	Diaphyseal (mm)
1	0.32 (91%)	0.29 (99%)	0.62 (78%)	0.19 (100%)
2	0.37 (95%)	0.34 (99%)	0.62 (81%)	0.27 (100%)
3	0.48 (93%)	0.36 (99%)	1.11 (61%)	0.34 (100%)
4	0.29 (97%)	0.35 (97%)	0.38 (92%)	0.16 (100%)
5	0.31 (97%)	0.30 (98%)	0.54 (86%)	0.22 (100%)
6	0.36 (97%)	0.38 (95%)	0.40 (81%)	0.37 (98%)
7	0.48 (88%)	0.43 (93%)	0.78 (69%)	0.37 (92%)
8	0.34 (97%)	0.46 (92%)	0.32 (98%)	0.26 (100%)

Figure 1

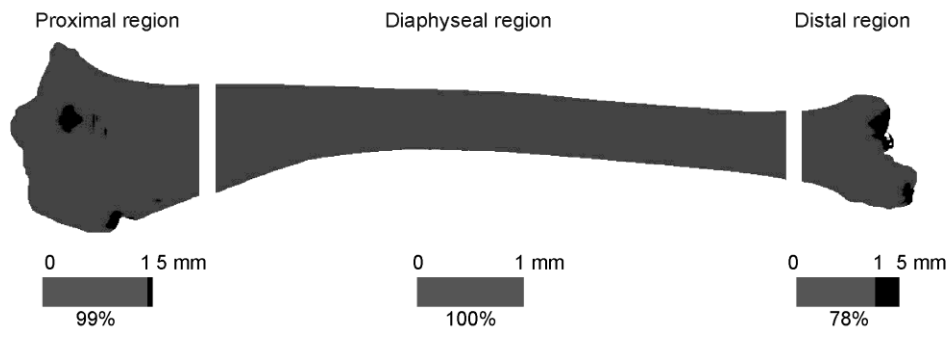


Figure 2

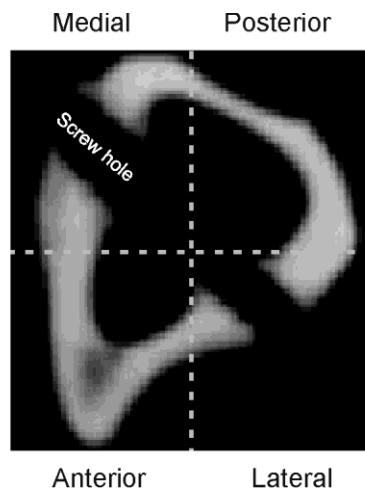
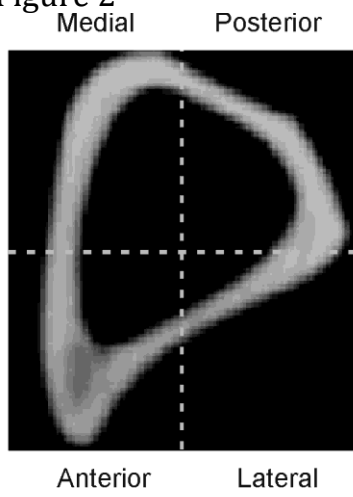


Figure 3

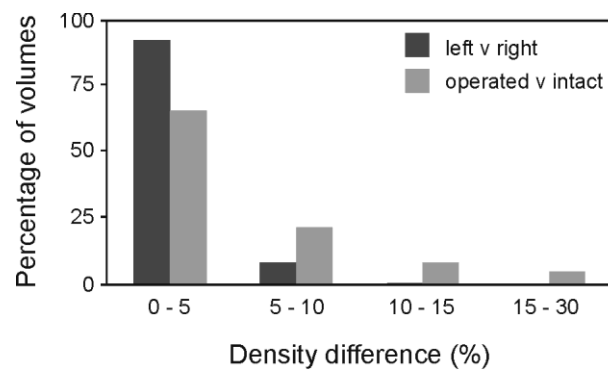


Figure 4

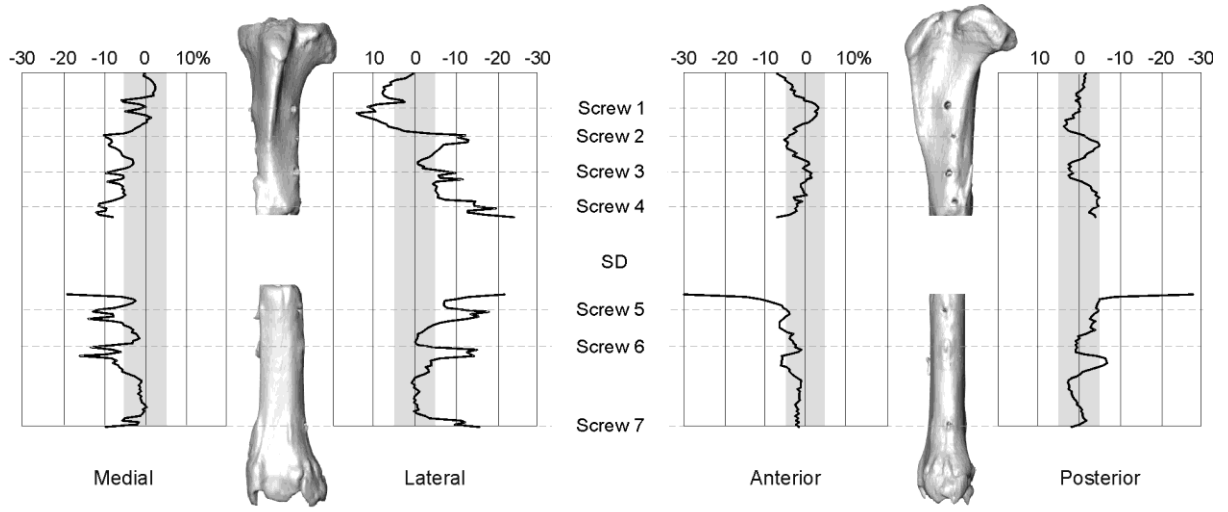


Figure 5

